ACS OMEGA

http://pubs.acs.org/journal/acsodf

Article

Characteristics, Accumulation, and Potential Health Risks of Antimony in Atmospheric Particulate Matter

Jiali Jiang,[#] Yunjie Wu,[#] Guangyi Sun,[*] Leiming Zhang, Zhonggen Li, Jonas Sommar, Heng Yao, and Xinbin Feng[*]

Cite This: *ACS Omega* 2021, 6, 9460−9470

Read Online

ACCESS | Metrics & More | Article Recommendations | Supporting Information

ABSTRACT: Antimony (Sb), a priority pollutant listed by the U.S. Environmental Protection Agency (USEPA), can cause adverse effects on human health, with particular impacts on skin, eyes, gastrointestinal tract, and respiratory system. In this study, a database of Sb concentrations in the global atmosphere was developed through a survey of measurements published in more than 600 articles, which was then used to assess the health risks of Sb exposure based on a USEPA assessment model. Most measurements showed Sb concentrations of less than ∼10 ng m^{-3}, but those at several contaminated sites exhibited Sb concentrations of more than 100 ng m^{-3}. For measurements conducted in urban environments, Sb concentrations in the total suspended particles (TSP) and particles of less than 10 (PM_{10}) or 2.5 μm ($PM_{2.5}$) were the highest in Asia, followed by Europe, South America, and North America. Sb concentrations were generally higher in winter and fall than during other seasons in TSP and PM_{10} samples. A significant correlation was observed between Sb and As in TSP and $PM_{2.5}$ on a global scale. Sb was mainly derived from anthropogenic sources, especially traffic emission, industrial emission, and fossil combustion. Hazard quotients (HQ) of Sb in TSP, PM_{10}, and $PM_{2.5}$ were higher for children than adults because of their lighter body weight, inferior physical resistance, and higher ingestion probability. The global database for atmospheric Sb concentrations demonstrates a relatively low noncarcinogenic risk in most regions. Long-term monitoring is still required to identify the sources and growth potentials of Sb so that effective control policies can be established.

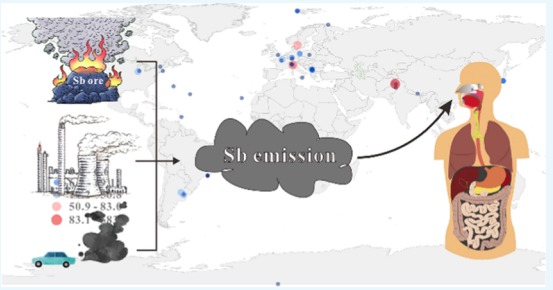

1. INTRODUCTION

Antimony (Sb) is the 51st element in the periodic table. Similar to other pnictogen atoms, Sb forms a volatile, highly toxic trihydride Sb^{3+} species, which is unstable under anaerobic conditions. The valence states of Sb in biological and environmental samples, however, are nearly entirely +III and +V.[1] Antimony can be bioaccumulated and harmful to creatures and is thus listed as a priority pollutant by the U.S. Environmental Protection Agency (USEPA) and the European Union.[2,3] The atmosphere serves as an important reservoir of Sb during its biogeochemical cycle. Anthropogenic Sb emissions have substantially increased the total Sb concentrations in the environment,[4−6] with current levels that are 50−100 times higher than the preindustrial era.[4] A 50% annual increase in the atmospheric Sb concentration in the northern hemisphere has been observed since the mid-1970s.[7] Anthropogenic Sb emissions to the atmosphere are particularly large in China (estimated to be 649 tons in 2010), accounting for 34% of global emissions.[8]

Airborne Sb generally exists in trace concentrations of pg m^{-3} to ng m^{-3} and has an atmospheric lifetime of hours to weeks, depending on its size distribution.[9] Most Sb emissions are from high-temperature combustion processes and are therefore released as submicron diameter particles, which can grow rapidly via accumulation in a bulk mode, represented by $PM_{2.5}$.[6] Particles in this size range can experience long-distance transport owing to their low dry and wet removal processes.[10,11] For example, Sb observed in the Canadian high Arctic almost entirely (99.8%) originates from anthropogenic emissions.[12]

Human exposure to Sb can be through breath, eat, drink, and skin contact. The toxicity posed by Sb to a human body depends on the exposure dose, duration, and routes, as well as the person's age, gender, nutritional status, family characteristics, lifestyle, and physical condition.[13] According to the Agency for Toxic Substances and Disease Registry,[14] chronic exposure to airborne Sb at a concentration of as low as 9 mg m^{-3} will exacerbate irritation in eyes, skin, and lungs. The reported minimal lethal doses for oral ingestion of Sb in the form of potassium antimony tartrate by children and adults are 300 and 1200 mg, respectively.[15] In addition, prolonged

Received: December 17, 2020
Accepted: March 22, 2021
Published: April 1, 2021

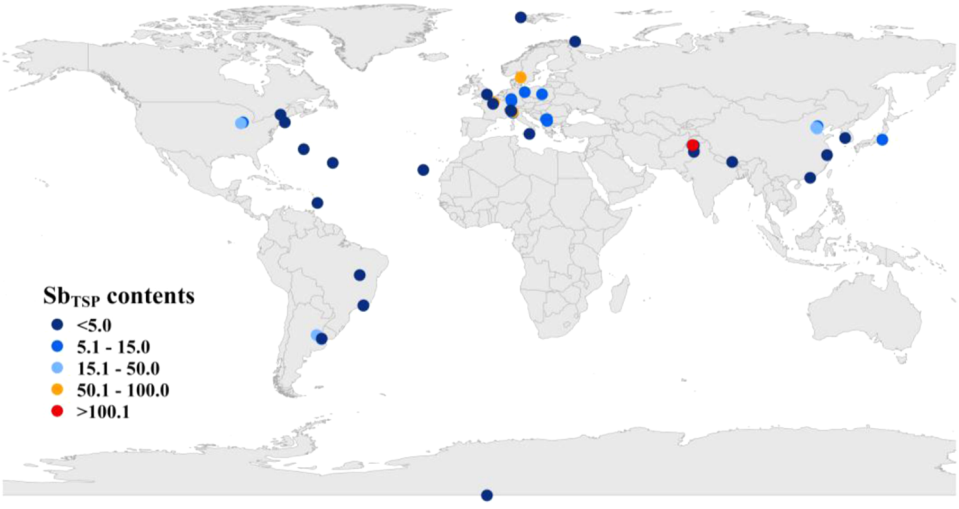

Figure 1. Global atmospheric Sb concentrations in TSP (ng m^{-3}).

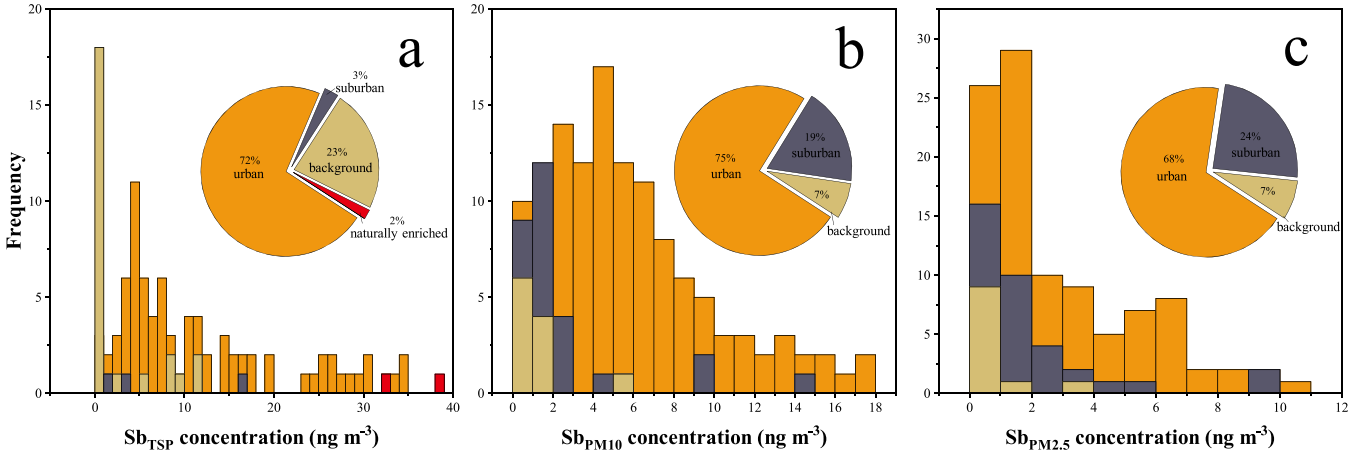

Figure 2. Distribution of atmospheric Sb concentrations by contamination class: (a) Sb$_{TSP}$ (Sb in total suspended particles), (b) Sb$_{PM10}$ (Sb in particles of less than 10 μm), and (c) Sb$_{PM2.5}$ (Sb in particles of less than 2.5 μm).

exposure to atmospheric Sb and Sb compounds can cause sleeplessness, electrocardiogram changes, stomachache, diarrhea, emesis, and gastric ulcers.[13,16−20] Chronic exposure to airborne dust containing a high proportion of antimony trioxide and antimony pentoxide has also caused pneumoconiosis.[21,22] However, assessments of the health risks caused by Sb exposure are still limited. Li et al.[23] reported that Sb exposure through oral ingestion exceeded the hazard quotient (HQ) safety level in Sb mining areas. Wu et al.[24] showed that dietary exposure to Sb was the dominant health risk to local residents in the largest Sb mining area in the world (Xikuangshan, Hunan province, China).

Antimony is a hazardous element closely related to human activities on a global scale. Large amounts of Sb have been released into various environment media by widespread human activities; thus, anthropogenic sources play a vital role in increasing Sb contents. Most existing studies have focused on Sb in various environmental media or in specific regions.[2,4,25−30] A systematic review of the global Sb distribution, its exposure assessment, and health risk characterization are still lacking. This study summarizes the published data of Sb concentrations in total suspended particles (TSPs) and size-segregated fractions (e.g., PM_{10} and $PM_{2.5}$) and assesses their potential health risks to humans. Results from the present study provide the much-needed knowledge for establishing a comprehensive atmospheric Sb cycle model, providing a reference for formulating future control policies and identifying future research needs.

2. RESULTS AND DISCUSSION

2.1. Global Distribution of Sb Concentrations. A total of 676 measurements of Sb concentrations in surface air were obtained from the literature; these were used to develop three data sets for Sb concentrations in TSP, PM_{10}, and $PM_{2.5}$ (Table S1). The majority of the data points were for urban and suburban environments, with only a few for background ambient air. Numerous studies have focused specifically on street canyons, tunnels, or other urban environments that are strongly impacted by traffic emissions. We note that not every study has TSP sampling, instead, only a fraction of the particulate mass was analyzed (e.g., $PM_{2.5}$, PM_{10}, and/or $PM_{10}-PM_{2.5}$). Only 532 measurements contained Sb concentrations in all of the TSP, PM_{10}, and $PM_{2.5}$, and these data were suitable for comparison. Data at different locations were used to generate spatial distribution figures.

Overall, Sb in TSP, PM_{10}, and $PM_{2.5}$ exhibited abnormal distributions (Shapiro−Wilk's test, $p < 0.01$), with profound positive skewness (Figure S1). We thus used the median values

https://doi.org/10.1021/acsomega.0c06091
ACS Omega 2021, 6, 9460−9470

of the concentration for comparison (Table S2). The median global Sb concentrations in TSP, PM_{10}, and $PM_{2.5}$ were 6.45, 4.00, and 1.43 ng m^{-3}, respectively. The standard deviations (SD) were large, indicating substantial data dispersion that reflects the large differences between sampling sites. The coefficient of variation decreased as follows: Sb_{TSP} > $Sb_{PM2.5}$ > Sb_{PM10}. This indicates that the Sb_{TSP} values had the highest degree of dispersion, followed by $Sb_{PM2.5}$ and then Sb_{PM10}. Detailed features and the spatial distributions of atmospheric Sb in TSP, PM_{10}, and $PM_{2.5}$ are discussed below.

2.1.1. Sb in TSP. Sampling sites were unevenly distributed around the world (Figure 1), with the majority of the sites in Europe (40%) and Asia (30%), followed by South America (13%), North America (8%), the Atlantic (8%), and Antarctica (2%). Antimony data from urban sites on four continents with evenly distributed data points were compared (Table S3); the highest Sb concentrations occurred in Asia, followed by Europe, South America, and North America. In general, Sb in TSP reflected the characteristics of local to regional atmospheric particulate Sb matter due to the relatively short transport distance of TSP.[9]

In this study, we grouped the measurement data into four main categories based on site characteristics: urban, suburban, background, and naturally enriched sites (Figure 2). Most of the data were obtained from urban sites, where Sb concentrations ranged from 0.035 to 40 ng m^{-3}. Background sites accounted for 23% of the data, where Sb concentrations were typically on the order of 0.1 ng m^{-3}. Only 3 and 2% of the data were collected at suburban and naturally enriched sites, respectively, with Sb concentrations ranging from 1 to 16 and 32 to 38 ng m^{-3}, respectively. As shown in Figure 1, the highest value of atmospheric Sb content in TSP was 583.8 ng m^{-3} in Wah Cantt, Pakistan,[31] a typical industrial city.

The distribution of the duration of measurements was also skewed, with 59% of the data points characterized by multiseason measurements and smaller portions by only single-season measurements (Figure S2). The sampling time was generally 24 h or longer.

2.1.2. Sb in PM_{10}. Sampling sites for Sb in PM_{10} were unevenly distributed among the continents, with 66% in Europe, 27% in Asia, and only 2, 1, and 4% in Africa, South America, and North America, respectively (Figure S3). Most samples were collected in urban (75%) or suburban areas (19%) and only 7% at background sites. A tendency can be observed in Table S3, where Sb levels decrease as follows: Asia > Europe > South America > North America. Besides, Sb_{PM10} concentrations ranged from 0 to 18 ng m^{-3} at urban sites, 0 to 14 ng m^{-3} at suburban sites, and 0 to 6 ng m^{-3} at background sites (Figure 2). The largest Sb value was 640 ng m^{-3} in Dachang, Guangxi Zhuang Autonomous Region, China,[32] which is named "the township of the nonferrous metal."

A heterogeneous temporal distribution was also observed, according to both the sampling season and collection time of the data (Figure S2). Nearly half of the studies collected samples during multiple seasons. More than half of the data were collected in both the daytime and nighttime. Several of the abovementioned temporal variabilities in Sb_{PM10} concentrations may originate from different sampling durations and measurement uncertainties (see Section 2.5).

2.1.3. Sb in $PM_{2.5}$. Sampling sites for $Sb_{PM2.5}$ were unevenly distributed among the continents (Figure S4), with 42, 29, 24, 4, and 1% in Europe, North America, Asia, South America, and Africa, respectively. $Sb_{PM2.5}$ decreased as follows: Asia > North America > Europe > South America (Table S3). This trend slightly differs from that shown in Mamun et al.,[33] who found higher Sb concentrations in Europe than North America. Such a difference may reflect the diverse data sources used in these two studies.

$Sb_{PM2.5}$ samples were predominantly collected from urban sites (68%), followed by suburban sites (24%) and background sites (7%). $Sb_{PM2.5}$ contents ranged from 0 to 11, 0 to 10, and 0 to 4 ng m^{-3} at urban, suburban, and background sites, respectively (Figure 2). The highest measured $Sb_{PM2.5}$ concentration was 516 ng m^{-3} in Korangi, Karachi, Pakistan,[34] which is one of the largest and most polluted metropolitan cities in South Asia.

Sampling time and season were also unevenly distributed (Figure S2). Most samples were collected during both the day and night. Sixty-one percent of the samples were collected in multiple seasons, where the most frequent sampling season was spring (19%), followed by summer (11%), autumn (3%), and winter (3%).

2.2. Factors Influencing Atmospheric Sb Concentrations. Global distributions of atmospheric Sb_{TSP}, Sb_{PM10}, and $Sb_{PM2.5}$ show that Sb concentrations are mostly below ~10 ng m^{-3} (Table S1), which is significantly less than the occupational standard level set by the U.S. Occupational Safety and Health Administration (OSHA), i.e., exposure for 8 h day^{-1} and 5 days $week^{-1}$ at a level of up to 0.5 mg m^{-3}. The highest Sb levels were associated with mining, industrial activities, automobile emissions, and coal mining activities (i.e., anthropogenic activities).

The impact of anthropogenic activities can influence the atmospheric Sb concentration. In TSP, PM_{10}, and $PM_{2.5}$ samples, except for naturally enriched areas, Sb concentrations varied at the different types of sampling sites (Kruskal–Wallis test, $p < 0.001$) in the following order: urban sites > suburban sites > background sites (Figure S5). This reflected the extent of the impacts of anthropogenic activities, with higher Sb concentrations from greater impacts.

Significant temporal variations were observed in the atmospheric Sb contents in TSP, PM_{10}, and $PM_{2.5}$ samples. The Sb data in different seasons were collected from our data set to analyze the influence of the season on Sb. Due to the sufficient amount of data, the priority was to analyze the Sb contents in urban areas. As shown in Figure 3, the Sb concentration for TSP decreased as follows: fall > winter > spring >summer. Significant seasonal differences also existed in Sb_{PM10} contents, e.g., fall > winter > summer > spring. $Sb_{PM2.5}$ levels decreased as follows: fall > summer > spring > winter. The higher Sb concentrations in winter and fall than in spring and summer were likely due to more coal consumption and lower mixing height during colder seasons.[35] More studies are required to verify these findings and identify the causes of inconsistencies of seasonal trends.

Antimony was typically enriched in small particles. The ratio of $Sb_{PM2.5}/Sb_{PM10}$ substantially exceeded 50% in the reported data,[36−44] suggesting significant Sb enrichment in fine particles. Furthermore, the mass median aerodynamic diameter (MMAD) of airborne Sb was 0.6 μm, which also indicates that Sb tends to concentrate in fine particles.[33] For example, Almeida et al.[43] observed a $Sb_{PM2.5}/Sb_{PM2.5-10}$ ratio of 1.6 (equivalent to $Sb_{PM2.5}/Sb_{PM10}$ of 61.5%) from samples collected in Bobadela on the western coast of Europe. Fujiwara et al.[28] found enriched Sb in the smallest particle sizes in road dust samples collected in Buenos Aires. Wang et al.[45] reported

https://doi.org/10.1021/acsomega.0c06091
ACS Omega 2021, 6, 9460−9470

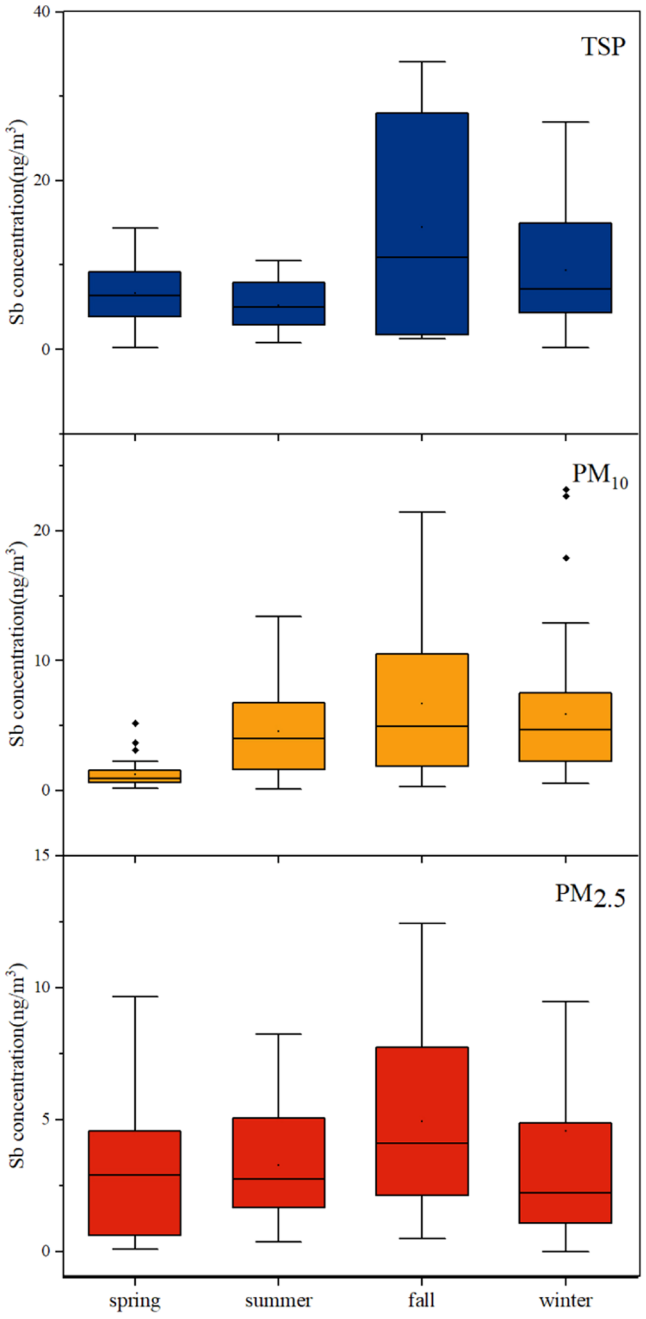

Figure 3. Boxplots of seasonal variations in airborne Sb contamination (the data derived from the literature listed in the Supporting Information[1,3,5−15,17−35,38−48,50,51,53]). The boxes represent the interquartile range (IQR) while the horizontal lines represent the maximum, median, and minimum values. The dots inside the boxes are average values, and the circles above the box are outliers.

the highest Sb content in the size range from 0.006 to 0.847 μm in Zhengzhou, China. Gómez et al.[46] observed enriched Sb (by a factor of 6.26) in the smallest size fraction of the Copahue volcanic ash. Furuta et al.[47] claimed that the smallest airborne particulate matter, with a diameter of less than 2 μm, has the highest Sb concentration.

Comparing data at a large number of background sites may reveal dominant variables that affect the total amount of atmospheric Sb. The data set developed in this study is inadequate for such analysis due to the limited background sites. Future research may fill this data gap.

2.3. Source Identification. The enrichment factor (EF) was initially developed to speculate on the origin of elements in the atmosphere, precipitation, or seawater,[48,49] and is now commonly used to identify and quantify human interference with global element cycles.[50] The formula to calculate EF can be generalized as[49]

$$\mathrm{EF} = \frac{[\mathrm{El}]_{\mathrm{sample}}/[\mathrm{X}]_{\mathrm{sample}}}{[\mathrm{El}]_{\mathrm{crust}}/[\mathrm{X}]_{\mathrm{crust}}}$$

where "El" is the element under consideration, "X" is the chosen reference element, and the square brackets indicate the concentration. The most commonly used reference elements are Al, Fe, Sc, and Ti for their little variabilities. In this study, Fe is used as the reference element to calculate EF for it is widely present in collected research studies. The concentrations of Sb and Fe in the crust are 43 200 and 0.3 μg/g, respectively.[51] EF > 5 indicates that the element may have a significant fraction contributed by noncrustal sources. High EF values were linked with the anthropogenic source of elements.[50]

As shown in Figure S6 and Table S4, the highest EF values were 56 000, 48 000, and 48 000, and the lowest ones were 33.6, 74.24, and 102.86 for TSP, PM_{10}, and $PM_{2.5}$, respectively. Most of EF values in the global atmosphere were higher than 100 and in the range of 100−1000; even the lowest EF values were still higher than 10, which indicated that Sb was mainly derived from anthropogenic sources.

Airborne particulate matter was a heterogeneous combination of diverse pollutants with complex sources, which varied greatly with different regions in the world. Sb in airborne particles can be derived from both natural and anthropogenic sources,[28,52] as illustrated in Figure 4.

Figure 4 shows the frequency of different sources that emerged in the surveyed cities, which was calculated as the ratio of the number of cities that emerged as a certain source to the total number of surveyed cities. For all of TSP, PM_{10}, and $PM_{2.5}$, less than 3% of the surveyed cities experienced emissions originated from volcanoes, local soils, and sea salt.

Among human activities, traffic emission, mostly from brake wear, was the dominant source of Sb in TSP, PM_{10}, and $PM_{2.5}$, and 36.1, 53.9, and 52.1% of the surveyed cities reported this source. Sb was defined as one of the "traffic-related" elements, and Sb enrichment near the traffic site was confirmed in previous studies.[25,53,54] Sb was widely used in brake pads in the form of Sb_2S_3, which can be discharged into the atmosphere during brake wear.[55] Fossil fuel combustion also contributed to Sb pollution in 16.7, 11.5, and 14.6% of the surveyed cities. Tian et al. claimed that Sb emissions from coal combustion in China increased from 133.19 tons in 1980[56] to 491.92 tons in 2012,[57] with an average annual growth rate of 4.2%. Industrial emissions (e.g., power plants, metal-smelting industry, and chemical plants) as sources of Sb were reported in 16.7, 9.6, and 12.5% of the surveyed cities for TSP, PM_{10}, and $PM_{2.5}$, respectively. The percentage of Sb(V) of PM_{10} samples in the brass industry was 84−88%, confirming the industrial source of Sb.[30] Other anthropogenic sources including mining activities, waste incineration, and unidentified sources also contributed Sb to airborne particulates. Besides, e-waste production was also an important source of Sb in regions with highest Sb concentrations (e.g., Asia and Europe).[58] Effectively recycling Sb from electronic waste for reducing Sb emissions is required in future.[59]

https://doi.org/10.1021/acsomega.0c06091
ACS Omega 2021, 6, 9460−9470

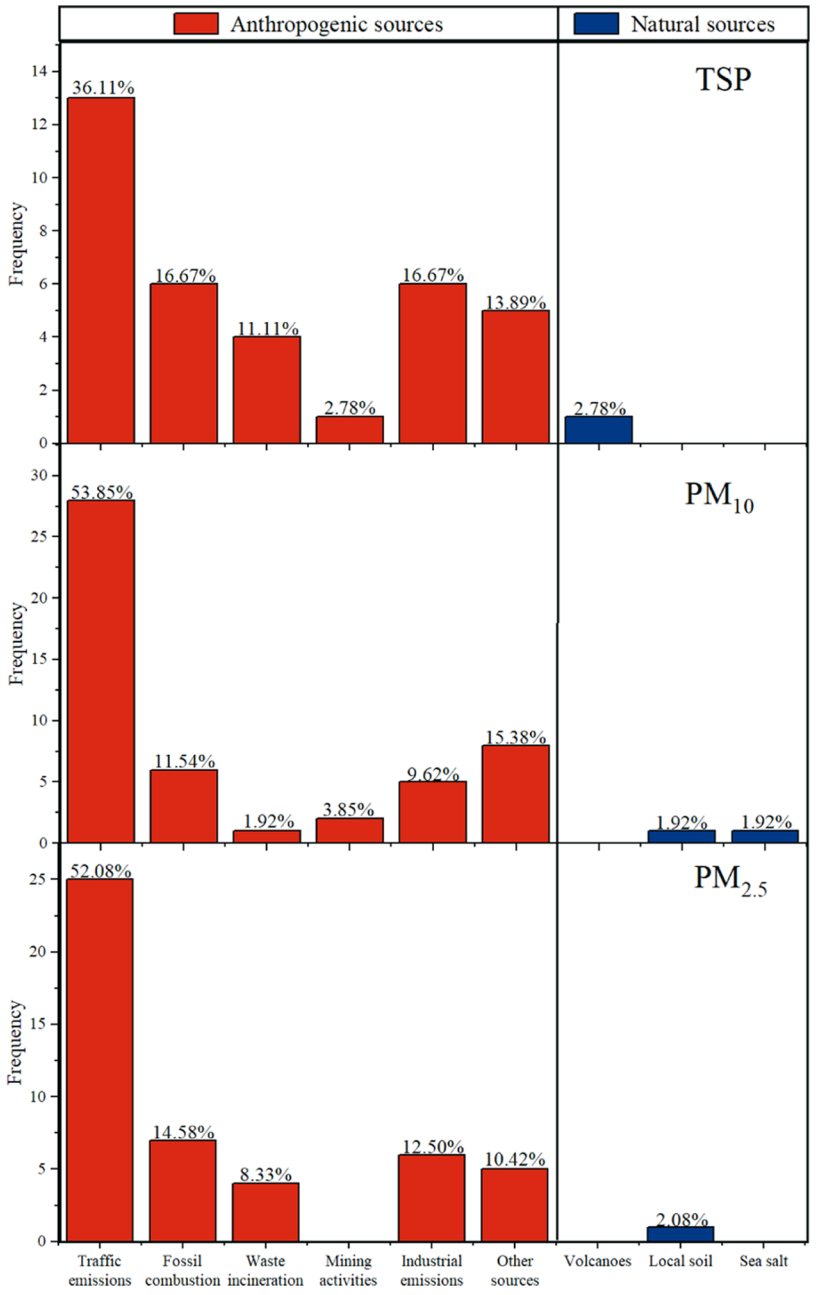

Figure 4. Major sources of airborne Sb contamination in surveyed cities.

The concentration ratio of Sb to some other trace elements can be used to determine the pollution sources of Sb. For example, a range of Sb/Se ratio was used to determine Sb sources from pyrometallurgical nonferrous metal production, refuse incineration, coal combustion, and marine biota.[60] A Cu/Sb ratio of 6.8 was referred to roadside sources, and a Cd/Sb ratio of 0.094 and Pb/Sb ratio of 6.8 were used as an indication of waste fly ash sources.[52] However, ratios generated from one city may not work properly in a different city due to the large heterogeneities of the sources between the different cities. A more accurate method for source identification, such as using isotope signatures, is urgently needed.

Overall, anthropogenic activities, particularly traffic emissions, fossil combustion, and industrial activities, were the dominant sources of Sb in TSP, PM_{10}, and $PM_{2.5}$. Reducing Sb emissions from these sources is crucial for lowering the Sb level in the global atmosphere and other related environmental media.

2.4. Human Health Risk Assessment of Global Atmospheric Sb. Numerous studies have confirmed the toxicity and bioavailability of Sb.[13,15−17] Antimony in the air affects human skin, eyes, gastrointestinal tract, and respiratory system.[61] There is, however, insufficient evidence to prove that Sb is carcinogenic in humans, despite the fact that studies have shown that antimony trioxide and antimony trisulfide cause lung tumors in rats.[62] Human carcinogenicity data for Sb are difficult to assess because of a subject's frequent and concurrent exposure to arsenic.[63] Hence, noncarcinogenicity was preferentially considered when assessing the health risks of Sb in the global atmosphere.

The average noncarcinogenic risk indices for adults and children from exposure to atmospheric Sb in the TSP, PM_{10},

https://doi.org/10.1021/acsomega.0c06091
ACS Omega 2021, 6, 9460−9470

and $PM_{2.5}$ fractions were calculated using eqs 1 and 2 (Figure 5). Based on the correlation between Sb and As, certain data

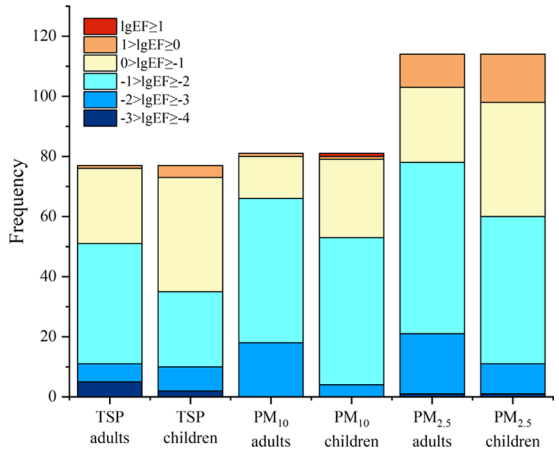

Figure 5. Frequency distributions of the hazard quotient values: Sb_{TSP}, Sb_{PM10}, and $Sb_{PM2.5}$.

derived from As contents were included in areas where atmospheric Sb studies were lacking. As listed in Table S5, the noncarcinogenic Sb risks for adults and children are significantly lower than 1 in most samples, despite the fact that children have higher HQ values than adults in the TSP, PM_{10}, and $PM_{2.5}$ samples. Children are more susceptible to noncarcinogenic effects than adults owing to their lower body weight, inferior physical resistance, and higher ingestion probability.[64] Besides, the differences in the HQ values between adults and children for the TSP, PM_{10}, and $PM_{2.5}$ samples were significant (Kruskal–Wallis test, $p = 0.005$, 0.006, $0.0014 < 0.05$).

Figure S7 shows the distribution of children's HQ values for the TSP fraction. The area with the highest HQ value was Wah Cantt, which is a typical industrial city in Pakistan,[31] but the HQ value did not exceed 1. For the PM_{10} fraction (Figure S7), the only region with an HQ value greater than 1 was Dachang, Guangxi Zhuang Autonomous Region, China (the township of the nonferrous metal and "the tin capital of China in the future").[32] For the $PM_{2.5}$ fraction (Figure S7), Karachi, Pakistan, one of the largest and most polluted metropolitan cities in South Asia,[34] had the highest HQ values, but these were still below 1. More detailed studies should be conducted at these sites to further investigate the adverse impact that Sb has on local residents.

According to the US-EPA guidelines, large HQ values above unity yield greater health concerns.[65] As shown in Figure 5, the majority of HQ values were less than 1, which indicates that atmospheric Sb has a relatively small noncarcinogenic effect in most areas. We note that the HQ value is only a simple measure of the possible impacts of Sb. The actual noncarcinogenic effects of Sb should be investigated via biological experiments.

To investigate the potential noncarcinogenic health risks of Sb, the HQ values of Sb in the TSP, PM_{10}, and $PM_{2.5}$ fractions were divided into several categories using exponential multiples. Values closer to 1 correspond to higher health risks and greater concerns. The distribution of the HQ values was different for children and adults so that we displayed the frequency distributions of the HQ values for Sb_{TSP}, Sb_{PM10}, and $Sb_{PM2.5}$ (Figure 5). The HQ values for atmospheric Sb in TSP ($p < 0.01$) and PM_{10} ($p = 0.04$) were not normally distributed, whereas the HQ values in the $PM_{2.5}$ fraction were normally distributed ($p = 0.07$) according to the Shapiro–Wilk's test. The main HQ values in the three size fractions, however, were predominantly distributed from 0.001 to 0.1, which indicates that most areas have a relatively low HQ level and health risk level.

2.5. Limitations and Uncertainties. The Sb database collected in this study was derived from available published data, which are not evenly distributed spatially or temporally. The focuses and measurement methods are not consistent among these studies, which may cause uncertainties in the generated global distribution of Sb and associated health concern analysis. For example, certain studies focused on spots with heavy Sb pollution, which may overestimate the Sb concentrations and exaggerate the human health risk if the data are used for regional-scale investigations. Removing abnormal values improved, to a certain extent, the accuracy of the spatial interpolation. In addition, the sources of Sb varied at different sites, such that the Sb speciation may be diverse. Currently, the correlation analysis approach is inadequate for evaluating the impact that different atmospheric Sb species have on human health.

Figure S8 summarizes information regarding the types of sampling devices, filters, and analytical techniques used in the publications analyzed in this study. For TSP measurements, high-volume cascade impactor samplers, cellulose membrane filters, and instrumental neutron activation analysis (INAA) were the most commonly used sampler, filter, and analytical instrument, respectively. For PM_{10} measurements, high-volume samplers, quartz filters, and inductively coupled plasma mass spectroscopy (ICP-MS) were most frequently used. For $PM_{2.5}$ measurements, poly(tetrafluoroethylene) (PTFE) and ICP-MS were the most popular filter and analytical technology, respectively, but sampling preferences were not consistent.

Tanaka et al.[66] found higher Sb concentrations in TSP obtained via INAA than LA-ICP-MS (Figure S9). Different filter materials also caused variations in Sb concentrations, as well as contributed substantially to blank values, especially the glass fiber filters.[67] Rizzio et al.[68] found that cellulose filters produced higher blank values than polycarbonate filters.

The reference values used in the exposure and health risk assessments may represent general trends but may not be suitable for certain situations in some areas. The selected reference values, i.e., ET, EF, ED, AT, IR, and RfD, can also produce uncertainties in the assessment results.

3. CONCLUSIONS AND RECOMMENDATIONS

This study developed a global database of atmospheric Sb concentrations and assessed its potential adverse impacts on humans. Antimony concentrations were predominantly less than ~10 ng m^{-3}, with the highest observed Sb_{TSP}, Sb_{PM10}, and $Sb_{PM2.5}$ concentrations at 583.8, 640, and 516 ng m^{-3}, respectively. Overall, field studies on TSP, PM_{10}, and $PM_{2.5}$ at Asian sites showed higher Sb concentrations than sites in Europe, South America, and North America. The sampling sites were unevenly distributed globally, with more than half of the Sb_{TSP} and Sb_{PM10} data collected in Europe and Asia, whereas most of the $PM_{2.5}$ data were collected in Europe, North America, and Asia. Higher Sb concentrations in TSP, PM_{10}, and $PM_{2.5}$ were observed in Asia than in Europe, South America, and North America. Higher Sb concentrations were also observed at urban and suburban sites than at background

https://doi.org/10.1021/acsomega.0c06091
ACS Omega 2021, 6, 9460–9470

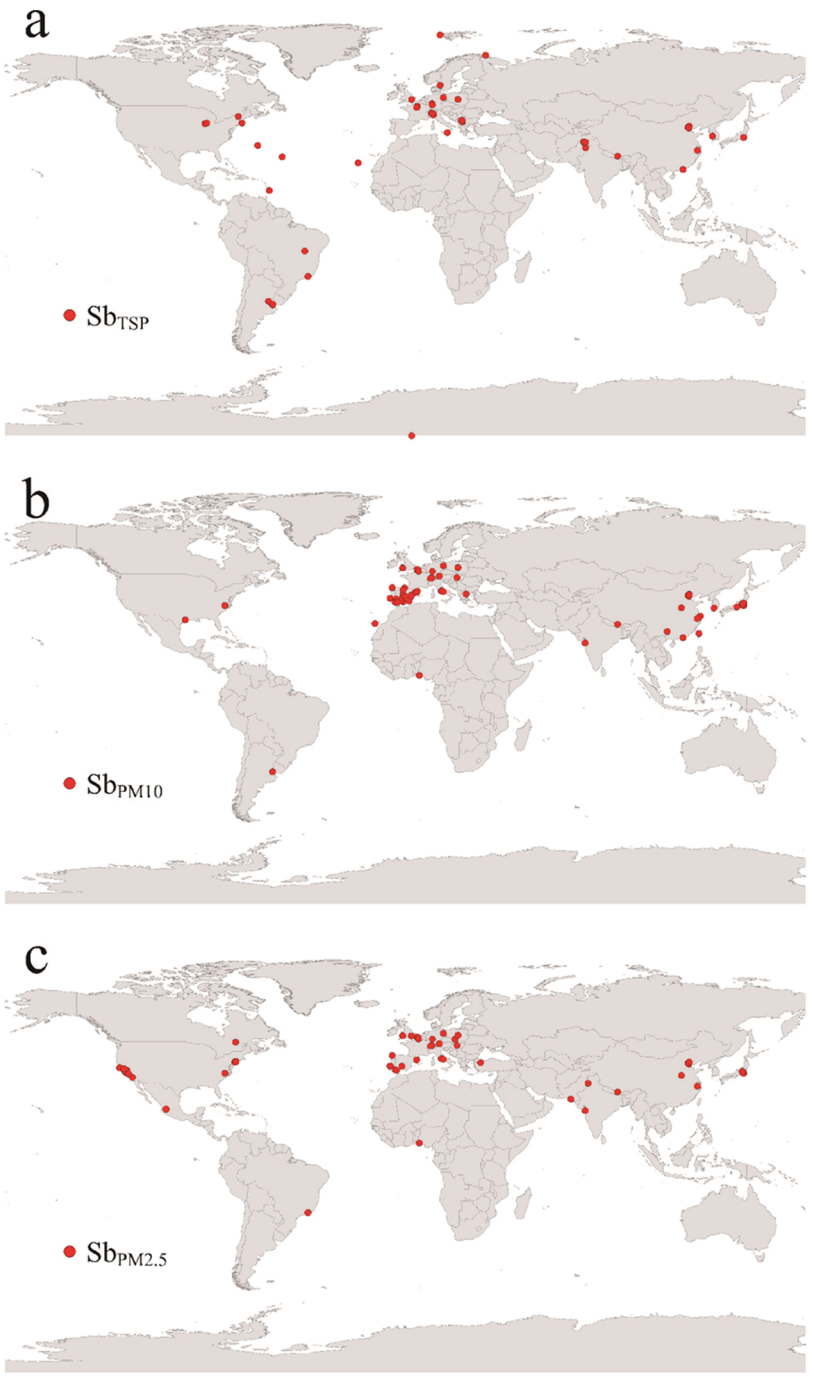

Figure 6. Sites of atmospheric Sb_{TSP} (a), Sb_{PM10} (b), and $Sb_{PM2.5}$ (c) monitoring data published in previous studies.

sites. Seasonal variation was obvious in TSP and PM_{10} samples since Sb contents were higher in fall and winter than spring and summer. Mass fractions of Sb were higher in $PM_{2.5}$ than TSP and PM_{10}. A significant correlation was observed between Sb and As in the TSP and $PM_{2.5}$ fractions, but the governing mechanism of this result requires further investigation. Source identification showed that Sb was mainly derived from anthropogenic sources, especially traffic emission (brake wear), industrial emission, and fossil combustion.

Global atmospheric Sb emissions from anthropogenic activities will increase to about 4000 t $year^{-1}$ by 2050 in the current legislation scenario,[66] with waste incineration and nonferrous metals production as major sources because of the population growth and expanding economics. More efficient PM control devices are needed to control Sb released into the atmosphere, for example, combining a electrostatic precipitator (ESP) or fabric filters (FFs) and recycling Sb from waste nonferrous metals products. Eventually, adjusting the existing energy structure and adopting clean energy are inevitable to reduce atmospheric Sb emissions.

In most areas, HQ values of Sb in the TSP, PM_{10}, and $PM_{2.5}$ fractions for both adults and children were less than 1, predominantly ranging from 0.001 to 0.1 in a non-normal distribution. HQ values were larger for children than adults with respect to Sb in the three size fractions, indicating higher noncarcinogenic risks for children than adults. The area with the highest Sb concentration had an HQ value greater than 1. Future field measurements should examine areas with sparse

https://doi.org/10.1021/acsomega.0c06091
ACS Omega 2021, 6, 9460−9470

data and reduce measurement uncertainties caused by different measurement techniques. More research is required to identify the dominant source factors of Sb and more reliably quantify its human health impacts.

4. MATERIALS AND METHODS

4.1. Data Collection and Processing. The literature published between 1970 and 2019 were surveyed to develop a database of Sb air concentrations. Data were acquired from published articles either by directly reading their data tables or digitization of their images using the Get data Graph Digitizer. Locations/areas with published atmospheric Sb data are shown in Figure 6 and listed in Table S1 (the sources of all data are given in references in SI). Most of the collected data comprise partially averaged and summarized values owing to limited research on atmospheric Sb and the fact that raw data for individual Sb concentrations were generally unreported in published studies.

To ensure the accuracy of large-scale spatial distributions, abnormal values outside the range of $(X/4, 4X)$ in the sampling data collected at the same location were removed, with X being the average Sb concentration of this location, because these values generally resulted from mining activities or artificial factors.[69] In addition, the data set included certain abnormally high values due to proximity to a pollution source. For this reason, we removed outliers that were more than 1.5 times the interquartile range (IQR) above the third quartile or below the first quartile. This procedure removed 19% of all data from the data set.

4.2. Risk Assessment Method. Risk exposure assessment procedures, according to US-EPA guidance,[70] consist of data collection, hazard identification, exposure parameter selection, and exposure estimation (see the detailed exposure model description below[71]). Atmospheric Sb mainly enters the human body via inhalation.[14] The natural defense mechanisms of the respiratory system excrete particles deposited in the tracheobronchial tree. Elements are divided into carcinogenic and noncarcinogenic ones based on the integrated risk information system (IRIS). Antimony has not undergone a complete evaluation regarding its human carcinogenic potential; therefore, HQ is preferred for assessing the health risks of Sb.

In accordance with the US-EPA exposure assessment model,[70] the chemical daily intake (CDI) was used to estimate the potential risks caused by Sb in airborne particulate matter via inhalation; the HQ was then calculated to assess noncarcinogenic risks from the above variables. The equations for these variables are as follows

$$\mathrm{CDI} = \frac{C \times \mathrm{IR} \times \mathrm{ET} \times \mathrm{EF} \times \mathrm{ED}}{\mathrm{BW} \times \mathrm{AT}} \quad (1)$$

$$\mathrm{HQ} = \frac{\mathrm{CDI}}{\mathrm{RfD} \times \frac{1000\ \mu\mathrm{g}}{\mathrm{mg}}} \quad (2)$$

where C ($\mu g\ m^{-3}$) is the Sb concentration in air, IR ($m^3\ day^{-1}$) is the inhalation rate, ET ($h\ day^{-1}$) is the exposure time, EF ($days\ year^{-1}$) is the exposure frequency, ED (years) is the exposure duration, BW (kg) is the average body weight, AT (lifetime in years × 365 days $year^{-1}$ × 24 h day^{-1}) is the average time, and RfD ($mg\ kg^{-1}\ day^{-1}$) is the reference dose. The exposure parameters used in eqs 1 and 2 are listed in Table S6.

Antimony and As both belong to group 15 in the periodic table, and they exhibit similar physical and chemical properties and geochemical behaviors. They often coexist in various environments.[72,73] In this study, a correlation between Sb and As was observed in airborne particulate matter, e.g., with a correlation coefficient of 0.51 ($p < 0.01$) in TSP and 0.64 ($p < 0.01$) in $PM_{2.5}$ (Figure S10). Considering that there are more studies available on As than Sb, certain preliminary information regarding Sb was inferred from As data in areas where atmospheric Sb data are absent or lacking to increase the amount of the atmospheric Sb concentration data used for health assessment analysis.

■ ASSOCIATED CONTENT

Supporting Information

The Supporting Information is available free of charge at https://pubs.acs.org/doi/10.1021/acsomega.0c06091.

The concentration of Sb in a global atmosphere; exposure parameters used in this study; concentrations of Sb in TSP, PM_{10}, and $PM_{2.5}$; regional urban Sb concentrations and median values in TSP, PM_{10}, and $PM_{2.5}$; EF of Sb in TSP, PM_{10}, and $PM_{2.5}$; hazard quotients of atmospheric Sb for adults and children in TSP, PM_{10}, and $PM_{2.5}$; comparison of Sb and As concentrations in TSP and $PM_{2.5}$; global atmospheric Sb concentrations in TSP, PM_{10}, and $PM_{2.5}$; boxplots of Sb concentrations at urban, suburban, and background sites; temporal, seasonal, and daily distributions of atmospheric Sb; global atmospheric Sb concentrations in PM_{10}; global atmospheric Sb concentrations in $PM_{2.5}$; frequency of EF of Sb in TSP, PM_{10}, and $PM_{2.5}$; noncarcinogenic hazard quotient values for Sb based on the TSP, PM_{10}, and $PM_{2.5}$ data; variability of sample devices, filters, and analytical techniques used for the Sb measurements; and a comparison of Sb analytical techniques (PDF)

■ AUTHOR INFORMATION

Corresponding Authors

Guangyi Sun − *State Key Laboratory of Environmental Geochemistry, Institute of Geochemistry, Chinese Academy of Sciences, Guiyang 550081, China;* orcid.org/0000-0001-8522-7973; Phone: +86-851-85895728; Email: sunguangyi@mail.gyig.ac.cn; Fax: +86-851-85891721

Xinbin Feng − *State Key Laboratory of Environmental Geochemistry, Institute of Geochemistry, Chinese Academy of Sciences, Guiyang 550081, China; CAS Center for Excellence in Quaternary Science and Global Change, Xi'an 710061, China;* orcid.org/0000-0002-7462-8998; Email: fengxinbin@vip.skleg.cn

Authors

Jiali Jiang − *State Key Laboratory of Environmental Geochemistry, Institute of Geochemistry, Chinese Academy of Sciences, Guiyang 550081, China; University of Chinese Academy of Sciences, Beijing 100049, China*

Yunjie Wu − *State Key Laboratory of Environmental Geochemistry, Institute of Geochemistry, Chinese Academy of Sciences, Guiyang 550081, China*

Leiming Zhang − *Air Quality Research Division, Science and Technology Branch, Environment and Climate Change*

https://doi.org/10.1021/acsomega.0c06091
ACS Omega 2021, 6, 9460−9470

Canada, Toronto M3H5T4, Canada; orcid.org/0000-0001-5437-5412

Zhonggen Li − *School of Resources and Environment, Zunyi Normal College, Zunyi 563006, China;* orcid.org/0000-0003-1408-5052

Jonas Sommar − *State Key Laboratory of Environmental Geochemistry, Institute of Geochemistry, Chinese Academy of Sciences, Guiyang 550081, China*

Heng Yao − *State Key Laboratory of Environmental Geochemistry, Institute of Geochemistry, Chinese Academy of Sciences, Guiyang 550081, China*

Complete contact information is available at: https://pubs.acs.org/10.1021/acsomega.0c06091

Author Contributions

[#]J.J. and Y.W. contributed equally to this work report.

Notes

The authors declare no competing financial interest.

■ ACKNOWLEDGMENTS

This study was funded by the National Key R&D Program of China (grant number 2020YFC1807700) and the China Postdoctoral Science Foundation (grant numbers 2018M640939 and 2020T130649).

■ REFERENCES

(1) Filella, M.; Williams, P. A.; Belzile, N. Antimony in the environment: knowns and unknowns. *Environ. Chem.* **2009**, *6*, 95−105.

(2) Gómez, D. R.; Fernanda Gine, M.; Claudia Sanchez Bellato, A.; Smichowski, P. Antimony: a traffic-related element in the atmosphere of Buenos Aires, Argentina. *J. Environ. Monit.* **2005**, *7*, 1162−1168.

(3) Seames, W. S.; Sooroshian, J.; Wendt, J. O. L. Assessing the solubility of inorganic compounds from size-segregated coal fly ash aerosol impactor samples. *J. Aerosol Sci.* **2002**, *33*, 77−90.

(4) Cloy, J. M.; Farmer, J. G.; Graham, M. C.; MacKenzie, A. B.; Cook, G. T. A comparison of antimony and lead profiles over the past 2500 years in Flanders Moss ombrotrophic peat bog, Scotland. *J. Environ. Monit.* **2005**, *7*, 1137−1147.

(5) Kuwae, M.; Tsugeki, N. K.; Agusa, T.; Toyoda, K.; Tani, Y.; Ueda, S.; Tanabe, S.; Urabe, J. Sedimentary records of metal deposition in Japanese alpine lakes for the last 250years: Recent enrichment of airborne Sb and In in East Asia. *Sci. Total Environ.* **2013**, *442*, 189−197.

(6) Shotyk, W.; Krachler, M.; Chen, B. Antimony in recent, ombrotrophic peat from Switzerland and Scotland: Comparison with natural background values (5320 to 8020 14C yr BP) and implications for the global atmospheric Sb cycle. *Global Biogeochem. Cycles* **2004**, *18* (1), 1−13.

(7) Heinrichs, H.; Brumsack, H.-J. *Anreicherung Von Umweltrelevanten Metallen in Atmosphärisch Transportierten Schwebstäuben Aus Ballungszentren, in Geochemie und Umwelt: Relevante Prozesse in Atmo-, Pedo- und Hydrosphäre*; Matschullat, J.; Tobschall, H. J.; Voigt, H.-J., Eds.; Springer: Berlin, Heidelberg, 1997; pp 25−36.

(8) Tian, H.; Zhou, J.; Zhu, C.; Zhao, D.; Gao, J.; Hao, J.; He, M.; Liu, K.; Wang, K.; Hua, S. A Comprehensive Global Inventory of Atmospheric Antimony Emissions from Anthropogenic Activities, 1995−2010. *Environ. Sci. Technol.* **2014**, *48*, 10235−10241.

(9) Seinfeld, J. H. P.; Spyros, N. *Atmospheric Chemistry and Physics: From Air Pollution to Climate Change*; Wiley: Hoboken, 2016.

(10) Gao, Y.; Nelson, E. D.; Field, M. P.; Ding, Q.; Li, H.; Sherrell, R. M.; Gigliotti, C. L.; Van Ry, D. A.; Glenn, T. R.; Eisenreich, S. J. Characterization of atmospheric trace elements on PM2.5 particulate matter over the New York−New Jersey harbor estuary. *Atmos. Environ.* **2002**, *36*, 1077−1086.

(11) Zhu, J.; Guo, J. Y.; Wang, L.; Pan, X.; Fu, Z.; Liao, H.; Fengchang, W. An overview of the environmental geochemistry of antimony. *Earth Environ.* **2010**, *38*, 109−116.

(12) Krachler, M.; Zheng, J.; Fisher, D.; Shotyk, W. Atmospheric Sb in the Arctic during the past 16,000 years: Responses to climate change and human impacts. *Global Biogeochem. Cycles* **2008**, *22* (1), 1−9.

(13) Cooper, R. G.; Harrison, A. P. The exposure to and health effects of antimony. *Indian J. Occup. Environ. Med.* **2009**, *13*, 3−10.

(14) Agency for Toxic Substances and Disease Registry, *Toxicological profile for antimony and compounds*; 1992.

(15) Herath, I.; Vithanage, M.; Bundschuh, J. Antimony as a global dilemma: Geochemistry, mobility, fate and transport. *Environ. Pollut.* **2017**, *223*, 545−559.

(16) Bingham, E.; Cohrssen, B.; Powell, C. *Patty's Toxicology*, 5th ed.; John Wiley & Sons, Inc.: New York, 2001; Vol. *1-9*.

(17) Brieger, H.; Semisch, C. W., 3rd; Stasney, J.; Piatnek, D. A. Industrial antimony poisoning. *Ind. Med. Surg.* **1954**, *23*, 521−523.

(18) Renes, L. E. Antimony poisoning in industry. *AMA Arch. Ind. Hyg. Occup. Med.* **1953**, *7*, 99−108.

(19) Scinicariello, F.; Buser, M. C.; Feroe, A. G.; Attanasio, R. Antimony and sleep-related disorders: NHANES 2005−2008. *Environ. Res.* **2017**, *156*, 247−252.

(20) Taylor, P. J. Acute intoxication from antimony trichloride. *Occup. Environ. Med.* **1966**, *23*, 318−321.

(21) Cooper, D. A.; Pendergrass, E. P.; Vorwald, A. J.; Mayock, R. L.; Brieger, H. Pneumoconiosis among worker in an antimony industry. *Am. J. Roentgenol.* **1968**, *103*, 495−508.

(22) Potkonjak, V.; Pavlovich, M. Antimoniosis: A particular form of pneumoconiosis. *Int. Arch. Occup. Environ. Health* **1983**, *51*, 199−207.

(23) Li, J.; Wei, Y.; Zhao, L.; Zhang, J.; Shangguan, Y.; Li, F.; Hou, H. Bioaccessibility of antimony and arsenic in highly polluted soils of the mine area and health risk assessment associated with oral ingestion exposure. *Ecotoxicol. Environ. Saf.* **2014**, *110*, 308−315.

(24) Wu, F.; Fu, Z.; Liu, B.; Mo, C.; Chen, B.; Corns, W.; Liao, H. Health risk associated with dietary co-exposure to high levels of antimony and arsenic in the world's largest antimony mine area. *Sci. Total Environ.* **2011**, *409*, 3344−3351.

(25) Dietl, C.; Reifenhäuser, W.; Peichl, L. Association of antimony with traffic — occurrence in airborne dust, deposition and accumulation in standardized grass cultures. *Sci. Total Environ.* **1997**, *205*, 235−244.

(26) Zheng, J.; Ohata, M.; Furuta, N. Antimony Speciation in Environmental Samples by Using High-Performance Liquid Chromatography Coupled to Inductively Coupled Plasma Mass Spectrometry. *Anal. Sci.* **2000**, *16*, 75−80.

(27) Filella, M.; Belzile, N.; Chen, Y.-W. Antimony in the environment: a review focused on natural waters: I. Occurrence. *Earth-Sci. Rev.* **2002**, *57*, 125−176.

(28) Fujiwara, F.; Rebagliati, R. J.; Marrero, J.; Gómez, D.; Smichowski, P. Antimony as a traffic-related element in size-fractionated road dust samples collected in Buenos Aires. *Microchem. J.* **2011**, *97*, 62−67.

(29) Quiroz, W.; Astudillo, F.; Bravo, M.; Cereceda-Balic, F.; Vidal, V.; Palomo-Marín, M. R.; Rueda-Holgado, F.; Pinilla-Gil, E. Antimony speciation in soils, sediments and volcanic ashes by microwave extraction and HPLC-HG-AFS detection. *Microchem. J.* **2016**, *129*, 111−116.

(30) Sánchez-Rodas, D.; Alsioufi, L.; Sánchez de la Campa, A. M.; González-Castanedo, Y. Antimony speciation as geochemical tracer for anthropogenic emissions of atmospheric particulate matter. *J. Hazard. Mater.* **2017**, *324*, 213−220.

(31) Nazir, R.; Shaheen, N.; Shah, M. H. Indoor/outdoor relationship of trace metals in the atmospheric particulate matter of an industrial area. *Atmos. Res.* **2011**, *101*, 765−772.

(32) Zhang, X. Y.; Tang, L. S.; Zhang, G.; Wu, H. D. Heavy metal contamination in a typical mining town of a minority and mountain area, South China. *Bull. Environ. Contam. Toxicol.* **2009**, *82*, 31−38.

(33) Al Mamun, A.; Cheng, I.; Zhang, L.; Dabek-Zlotorzynska, E.; Charland, J.-P. Overview of size distribution, concentration, and dry deposition of airborne particulate elements measured worldwide. *Environ. Rev.* **2019**, 1−12.
(34) Lurie, K.; Nayebare, S. R.; Fatmi, Z.; Carpenter, D. O.; Siddique, A.; Malashock, D.; Khan, K.; Zeb, J.; Hussain, M. M.; Khatib, F.; et al. PM2.5 in a megacity of Asia (Karachi): Source apportionment and health effects. *Atmos. Environ.* **2019**, *202*, 223−233.
(35) Janhäll, S.; Olofson, K. F. G.; Andersson, P. U.; Pettersson, J. B. C.; Hallquist, M. Evolution of the urban aerosol during winter temperature inversion episodes. *Atmos. Environ.* **2006**, *40*, 5355−5366.
(36) Fukai, T.; Kobayashi, T.; Sakaguchi, M.; Aoki, M.; Saito, T.; Fujimori, E.; Haraguchi, H. Chemical characterization of airborne particulate matter in ambient air of Nagoya, Japan, as studied by the multielement determination with ICP-AES and ICP-MS. *Anal. Sci.* **2007**, *23*, 207−213.
(37) Cho, S.-H.; Tong, H.; McGee, J. K.; Baldauf, R. W.; Krantz, Q. T.; Gilmour, M. I. Comparative Toxicity of Size-Fractionated Airborne Particulate Matter Collected at Different Distances from an Urban Highway. *Environ. Health Perspect.* **2009**, *117*, 1682−1689.
(38) Iijima, A.; Sato, K.; Ikeda, T.; Sato, H.; Kozawa, K.; Furuta, N. Concentration distributions of dissolved Sb(III) and Sb(V) species in size-classified inhalable airborne particulate matter. *J. Anal. At. Spectrom.* **2010**, *25*, 356−363.
(39) Tran, D. T.; Alleman, L. Y.; Coddeville, P.; Galloo, J.-C. Elemental characterization and source identification of size resolved atmospheric particles in French classrooms. *Atmos. Environ.* **2012**, *54*, 250−259.
(40) Moreno, T.; Alastuey, A.; Querol, X.; Font, O.; Gibbons, W. The identification of metallic elements in airborne particulate matter derived from fossil fuels at Puertollano, Spain. *Int. J. Coal Geol.* **2007**, *71*, 122−128.
(41) Duan, J.; Tan, J.; Wang, S.; Hao, J.; Chai, F. Size distributions and sources of elements in particulate matter at curbside, urban and rural sites in Beijing. *J. Environ. Sci.* **2012**, *24*, 87−94.
(42) Fan, X. B.; Liu, W.; Wang, G. H.; Lin, J.; Fu, Q. Y.; Gao, S.; Li, Y. Size distributions of concentrations and chemical components in Hangzhou atmospheric particles. *China Environ. Sci.* **2011**, *31*, 13−18.
(43) Almeida, S. M.; Pio, C. A.; Freitas, M. C.; Reis, M. A.; Trancoso, M. A. Source apportionment of fine and coarse particulate matter in a sub-urban area at the Western European Coast. *Atmos. Environ.* **2005**, *39*, 3127−3138.
(44) Avino, P.; Capannesi, G.; Rosada, A. Characterization and distribution of mineral content in fine and coarse airborne particle fractions by Neutron Activation Analysis. *Toxicol. Environ. Chem.* **2006**, *88*, 633−647.
(45) Wang, S.; Yan, Q.; Zhang, R.; Jiang, N.; Yin, S.; Ye, H. Size-fractionated particulate elements in an inland city of China: Deposition flux in human respiratory, health risks, source apportionment, and dry deposition. *Environ. Pollut.* **2019**, *247*, 515−523.
(46) Gómez, D.; Smichowski, P.; Polla, G.; Ledesma, A.; Resnizky, S.; Rosa, S. Fractionation of elements by particle size of ashes ejected from Copahue Volcano, Argentina. *J. Environ. Monit.* **2002**, *4*, 972−977.
(47) Furuta, N.; Iijima, A.; Kambe, A.; Sakai, K.; Sato, K. Concentrations, enrichment and predominant sources of Sb and other trace elements in size classified airborne particulate matter collected in Tokyo from 1995 to 2004. *J. Environ. Monit.* **2005**, *7*, 1155−1161.
(48) Goldberg, E. D. In *Baseline Studies of Pollutants in the Marine Environment: Heavy Metals, Halogenated Hydrocarbons and Petroleum*, Background Papers for a Workshop Sponsored by the National Science Foundation's Office for the International Decade of Oceanography; Brookhaven National Laboratory, 1972.
(49) Chester, R.; Stoner, J. H. Pb in Particulates from the Lower Atmosphere of the Eastern Atlantic. *Nature* **1973**, *245*, 27−28.
(50) Reimann, C.; Caritat, Pd. Intrinsic Flaws of Element Enrichment Factors (EFs) in Environmental Geochemistry. *Environ. Sci. Technol.* **2000**, *34*, 5084−5091.
(51) Hans Wedepohl, K. The composition of the continental crust. *Geochim. Cosmochim. Acta* **1995**, *59*, 1217−1232.
(52) Iijima, A.; Sato, K.; Fujitani, Y.; Fujimori, E.; Saito, Y.; Tanabe, K.; Ohara, T.; Kozawa, K.; Furuta, N. Clarification of the predominant emission sources of antimony in airborne particulate matter and estimation of their effects on the atmosphere in Japan. *Environ. Chem.* **2009**, *6*, 122−132.
(53) Zereini, F.; Alt, F.; Messerschmidt, J.; Wiseman, C.; Feldmann, I.; von Bohlen, A.; MÜller, J.; Liebl, K.; PÜttmann, W. Concentration and Distribution of Heavy Metals in Urban Airborne Particulate Matter in Frankfurt am Main, Germany. *Environ. Sci. Technol.* **2005**, *39*, 2983−2989.
(54) Smichowski, P. Antimony in the environment as a global pollutant: a review on analytical methodologies for its determination in atmospheric aerosols. *Talanta* **2008**, *75*, 2−14.
(55) Varrica, D.; Bardelli, F.; Dongarrà, G.; Tamburo, E. Speciation of Sb in airborne particulate matter, vehicle brake linings, and brake pad wear residues. *Atmos. Environ.* **2013**, *64*, 18−24.
(56) Tian, H. Z.; Zhao, D.; He, M. C.; Wang, Y.; Cheng, K. Temporal and spatial distribution of atmospheric antimony emission inventories from coal combustion in China. *Environ. Pollut.* **2011**, *159*, 1613−1619.
(57) Tian, H. Z.; Zhu, C. Y.; Gao, J. J.; Cheng, K.; Hao, J. M.; Wang, K.; Hua, S. B.; Wang, Y.; Zhou, J. R. Quantitative assessment of atmospheric emissions of toxic heavy metals from anthropogenic sources in China: historical trend, spatial distribution, uncertainties, and control policies. *Atmos. Chem. Phys.* **2015**, *15*, 10127−10147.
(58) Forti, V.; B, C. P.; Kuehr, R.; Bel, G. *The Global E-waste Monitor 2020: Quantities, Flows and the Circular Economy Potential*; United Nations University/United Nations Institute for Training and Research, International Telecommunication Union, and International Solid Waste Association: Bonn/Geneva/Rotterdam, 2020.
(59) Barragan, J. A.; Ponce de León, C.; Alemán Castro, J. R.; Peregrina-Lucano, A.; Gómez-Zamudio, F.; Larios-Durán, E. R. Copper and Antimony Recovery from Electronic Waste by Hydrometallurgical and Electrochemical Techniques. *ACS Omega* **2020**, *5*, 12355−12363.
(60) Arimoto, R.; Duce, R. A.; Savoie, D. L.; Prospero, J. M. Trace elements in aerosol particles from Bermuda and Barbados: Concentrations, sources and relationships to aerosol sulfate. *J. Atmos. Chem.* **1992**, *14*, 439−457.
(61) Sundar, S.; Chakravarty, J. Antimony Toxicity. *Int. J. Environ. Res. Public Health* **2010**, *7*, 4267−4277.
(62) Groth, D. H.; Stettler, L. E.; Burg, J. R.; Busey, W. M.; Grant, G. C.; Wong, L. Carcinogenic effects of antimony trioxide and antimony ore concentrate in rats. *J. Toxicol. Environ. Health* **1986**, *18*, 607−626.
(63) De Boeck, M.; Kirsch-Volders, M.; Lison, D. Cobalt and antimony: genotoxicity and carcinogenicity. *Mutat. Res., Fundam. Mol. Mech. Mutagen.* **2003**, *533*, 135−152.
(64) Ahmed, N.; Bodrud-Doza, M.; Towfiqul Islam, A. R. M.; Hossain, S.; Moniruzzaman, M.; Deb, N.; Bhuiyan, M. A. Q. Appraising spatial variations of As, Fe, Mn and NO3 contaminations associated health risks of drinking water from Surma basin, Bangladesh. *Chemosphere* **2019**, *218*, 726−740.
(65) USEPA, *Risk Assessment Guidance for Superfund Volume I: Human Health Evaluation Manual: Part A*, 1989.
(66) Tanaka, S.; Yasushi, N.; Sato, N.; Fukasawa, T.; Santosa, S. J.; Yamanaka, K.; Ootoshi, T. Rapid and simultaneous multi-element analysis of atmospheric particulate matter using inductively coupled plasma mass spectrometry with laser ablation sample introduction. *J. Anal. At. Spectrom.* **1998**, *13*, 135−140.
(67) Bem, H.; Gallorini, M.; Rizzio, E.; Krzemińska, M. Comparative studies on the concentrations of some elements in the urban air particulate matter in Lodz City of Poland and in Milan, Italy. *Environ. Int.* **2003**, *29*, 423−428.

https://doi.org/10.1021/acsomega.0c06091
ACS Omega 2021, 6, 9460−9470

(68) Rizzio, E.; Giaveri, G.; Gallorini, M. Some analytical problems encountered for trace elements determination in the airborne particulate matter of urban and rural areas. *Sci. Total Environ.* **2000**, *256*, 11−22.
(69) Zeng, S.; Ma, J.; Yang, Y.; Zhang, S.; Liu, G.-J.; Chen, F. Spatial assessment of farmland soil pollution and its potential human health risks in China. *Sci. Total Environ.* **2019**, *687*, 642−653.
(70) USEPA, *Risk Assessment Guidance for Superfund Volume I: Human Evaluation Manual: Part F, Supplemental Guidance for Inhalation Risk Assessment*, 2009.
(71) Stewart, P.; Stenzel, M. Exposure Assessment in the Occupational Setting. *Appl. Occup. Environ. Hyg.* **2000**, *15*, 435.
(72) IRIS, Antimony trioxide, CASRN 1309-64-4, 1995. https://cfpub.epa.gov/ncea/iris2/chemicalLanding.cfm?substance_nmbr=676 (accessed on Feb 2, 2021).
(73) USEPA, Update of Standard Default Exposure Factors, 2014. https://www.epa.gov/risk/update-standard-default-exposure-factors (accessed on Feb 2, 2021).

https://doi.org/10.1021/acsomega.0c06091
ACS Omega 2021, 6, 9460−9470